J Mater Sci (2007) 42:10160–10163
DOI 10.1007/s10853-007-2116-6

A study on electrodeposited $Zn_{1-x}Fe_x$ alloys

Ismail Hakki Karahan

Received: 2 April 2007 / Accepted: 14 August 2007 / Published online: 25 September 2007

Abstract $Zn_{1-x}Fe_x$ alloys were electrochemically deposited on AISI 4140 steel substrates from sulfate bath. The bath was consisted of 40 g dm^{-3} $ZnSO_4 \cdot 7H_2O$, 20–40 g dm^{-3} $FeSO_4 \cdot 7H_2O$, 25 g dm^{-3} $Na_3C_6H_5O_7$, and 16 g dm^{-3} H_3BO_3. The effect of bath composition on the electrical resistivity, the phase structure, and the corrosion behavior were investigated by the current–voltage measurements versus temperature, the X-ray diffraction (XRD) analysis, the atomic absorption spectrometry analysis, and the polarization measurements, respectively. Iron content was shown to strongly affect the structure, the electrical resistivity and the corrosion stability of Zn–Fe alloys.

Introduction

Electrodeposited zinc-alloy coatings and those especially containing one of the 'iron group metals' (e.g., iron, nickel, and cobalt) have found to be important end-uses in various industrial sectors. One of their subgroups, zinc–iron electrodeposited coatings on steel sheets comprise one of the most promising groups of materials for the automotive industry. The electrodeposited Zn–Fe alloy coatings posses many excellent properties, such as excellent corrosion resistance due to the nature of the zinc–iron phase, excellent paintability and good welding properties of zinc–iron phase in comparison to the pure zinc [1–4], and have been considered to be an alternative for the pure zinc coatings of iron and steel products. These are easily achieved by alloying Zn with more noble metals, mostly with metals of the iron group (Ni, Co, and Fe) [5, 6]. Zinc–iron alloys exist in various phases, and also their structure and morphology [7] also determine the corrosion resistance of a deposit. The electrodeposition of zinc alloys with the iron group metals are to be anomalously codeposited, whereby zinc—the less noble metal—is deposited preferentially. Anomalous codeposition is therefore a very important phenomenon in the electrodeposition of zinc alloys. Therefore, many research groups have reported the preparation of these alloys with high or low iron content, respectively [8–10].

The first objective of this study is to prepare Zn–Fe alloy coatings onto steel substrates in a useful form from a sulfate bath in the static-current conditions. The second objective is to study the influence of bath composition on electrical resistivity, corrosion resistance, composition and structure properties of Zn–Fe alloys.

Experimental

Electrodeposition of Zn–Fe alloys

$Zn_{1-x}Fe_x$ alloys were deposited from a sulfate plating bath consisted of 40 g dm^{-3} $ZnSO_4 \cdot 7H_2O$, 20–40 g dm^{-3} $FeSO_4 \cdot 7H_2O$, 25 g dm^{-3} $Na_3C_6H_5O_7$, and 16 g dm^{-3} H_3BO_3. The pH value of the bath was adjusted to about 4 with hydrochloric acid. The employed electrolyte was prepared using p.a. chemicals (Merck) and double distilled water. Depositions were carried out at a current density of 1 A dm^{-2}. Experimental temperature was 50 °C. The working electrodes (WE) used for electrodeposition were AISI 4140 steel disks and the chemical composition of AISI 4140 steel is given in Table 1. They were polished with silicon

I. H. Karahan (✉)
Department of Physics, Faculty of Art and Science,
University of Kilis 7 Aralık, Kilis, Turkey
e-mail: ikarahan@gantep.edu.tr

Table 1 Chemical composition of AISI 4140 low alloy steel (%)

Element	C	Mn	Si	Cr	Ni	Mo	V	S	Cu	P
Wt.%	0.36	0.80	0.005	0.914	0.30	0.85	0.075	0.07	0.143	0.034

carbide papers from 3 through 1 to 0.5 Am and velvet, rinsed with the twice distilled water, washed in acetone, rinsed with the twice distilled water again and then dried in air. Counter electrode was a Pt gauze electrode. The reference electrode used in all experiments was a saturated calomel electrode (SCE). The phases present in the deposits and the preferred orientation of the deposits were determined by X-ray diffraction (XRD) analysis, using a Siemens D500 X-ray diffractometer with CuK-α radiation. The 2θ range of 10–60° was recorded at a rate of 0.02° 2θ/0.5 s. The crystal phases were identified comparing the 2θ values and intensities. The compositions of the films shown in Table 2 were determined using an atomic absorption spectrophotometer.

Corrosion measurements

The electrochemical behaviors of the electrodeposited Zn–Fe alloys were analyzed in 3 wt.% NaCl aqueous solution at room temperature in a Pyrex glass cell. The corrosion behaviors of the samples were investigated by a potentiodynamic polarization technique. Polarization measurements were performed with an electrochemical analyzer/workstation (Model 1100, CH Instruments, USA) with a three-electrode configuration. The exposed area of the specimens were about 1 cm^2. The specimens were covered with a cold setting resin and immersed into the solution until a steady open circuit potential (ocp) was reached. After equilibration, polarization was started at a rate of 1 mV/s.

Electrical resistivity measurements

$Zn_{1-x}Fe_x$ alloys were prepared by the constant current technique. The deposition was performed with a current of 1 A/dm^2 at 50 °C and pH = 4. The films were deposited onto an aluminum substrate, which was subsequently stripped from the films by using 10% NaOH solution for electrical resistivity measurements. The resistivity measurements were done using the traditional four-point probe method. The thermal voltage effect was eliminated by taking the average of voltage readings with two reverse currents at each temperature. Each sample was measured several times to make sure the obtained data was reliable. A closed-cycle helium cryostat (Leybold RW2) was used to control the sample temperature with a sensitivity of ±0.2 K. Sample dimensions for the resistivity measurements were 1 mm × 4 mm × 4 × 10^{-4} mm.

Table 2 Chemical composition of bath and coatings

% at Electrolyte		% at Electrodeposits	
Zn	Fe	Zn	Fe
77	33.3	78	22
57.1	42.9	69	31
50	50	61	39

Results and discussion

Brenner [11] classified the electrodeposition of Zn–Fe alloys as anomalous. Codeposition of Zn and Fe is, however, not always anomalous since at low current densities, it is possible to obtain normal deposition, where Fe deposits preferentially to Zn.

Figure 1 shows the dependence of Fe deposit content on the bath $FeSO_4$ content (g dm^{-3}). It is clear from the figure that the Fe deposit content is measured to be 22 wt.% for the bath Fe concentration of 20 g dm^{-3} while the Zn content is obtained to be 80 wt.%. The increase in the Fe concentrations is caused by an increase of the Fe deposit content. But the Zn^{+2} ions are preferentially deposited more than the Fe^{+2} ions. This is obeyed to the phenomenon called 'anomalous codeposition' which was described as the preferential deposition of the element with less positive standard electrode potential [12].

Cyclic voltammetry was used to define the major characteristics of the zinc deposition process. Figure 2 shows the typical voltammograms obtained in the three solutions.

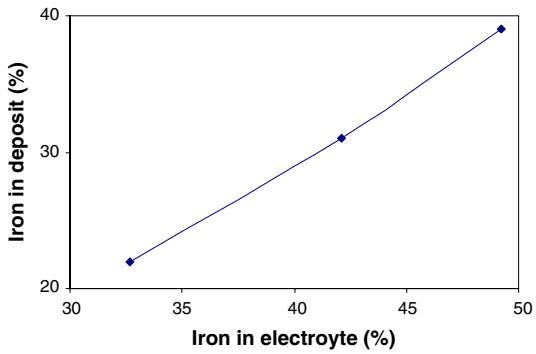

Fig. 1 Dependence of Fe content of the deposits on electrolyte Fe concentrations

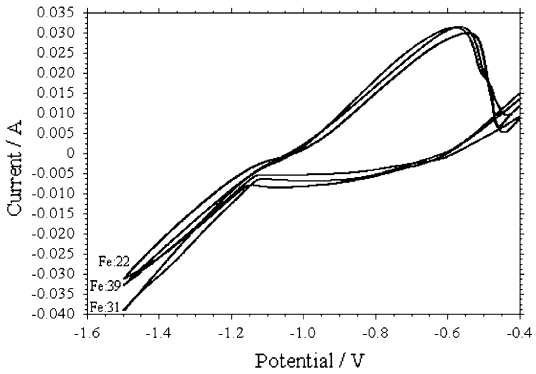

Fig. 2 Cyclic voltammograms for the Zn–Fe alloys

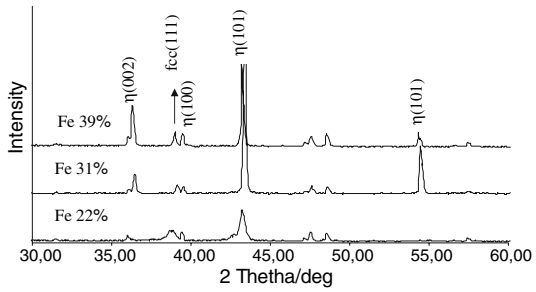

Fig. 3 The typical XRD pattern of the resulted Zn–Fe alloy coating

The scans were initiated at E = –400 mV. In solutions, during the forward scan towards the negative direction, the cathodic current increased sharply when the Zn–Fe deposition begins. The sign of a nucleation and growth process as current crossover is not observed [13].

Figure 3 demonstrates XRD patterns of the electrodeposited Zn–Fe alloys. The Zn–Fe alloy coatings have the same structure as zinc [2] but different crystallographic orientation, which is the consequence of the small iron amount. The phases of the electrodeposited Zn–Fe alloys are very complicated depending on the chemical compositions [14, 15]. The reflections of zinc-rich phase (JCP: 4-0831) [16] and a ζ phase are present in all investigated deposits. The electrodeposited Zn–Fe alloys have metastable structures and many phases coexist over a wide range of composition. Adaniya et al. [17] have reported that the phases of electrodeposited Zn–Fe alloys include: η phase (100–81% Zn), δ_1/γ phase (89–70% Zn), γ phase (87–48% Zn), and α phase (62–0% Zn). Only relative intensities of the two phases change among the deposited layers with different compositions. As the Zn content in the deposits increases the signals belonging to the η phase when it becomes more intense.

Figure 4 shows the temperature versus normalized resistivity values of the alloys. A linear change in the resistivity of Zn_xFe_{1-x} films with the variation of the Fe content from x = 22 to 39 could not be observed although

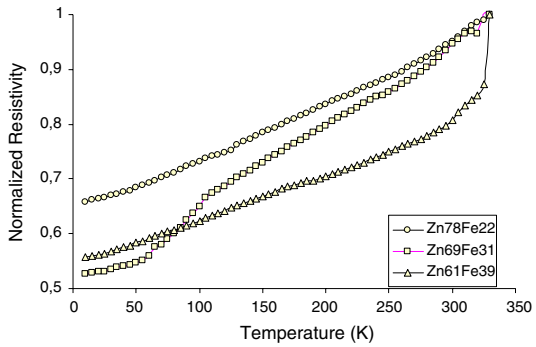

Fig. 4 Normalized resistivity curves as a function of temperature

the change in the resistivity with the variation of temperature is almost linear for all the three samples. The biggest resistivity was detected in the $Zn_{78}Fe_{22}$ film while the largest change in the resistivity with temperature was observed in the $Zn_{69}Fe_{31}$ alloy. $Zn_{61}Fe_{39}$ alloy shows a very sharp resistivity increase above 300 K. The temperature dependent resistivity curves in the figure appear not to obey Matthiessen's rule which predicts parallel temperature-dependent resistivity curves. However, the Kondo effect predicts a departure from the Matthiessen's rule in the samples with small magnetic atom contamination, e.g., Fe, in a non-magnetic metallic matrix, e.g., Zn and Cu. This anomalous behavior is due to an additional scattering of electrons by magnetic moments on the impurity centers [18]. The resistivity–temperature variation with Co content may therefore be much more complex than that implied by Matthiessen's rule. However, the decrease in the resistivity with decreasing temperature seems to be due to the reduction of the numbers of both phonons and magnons.

Zinc is a good anti-corrosive material and the fundamental function of iron in the coatings is to make the corrosion potential more positive. In this case, the alloy coatings become nobler than zinc coatings and the Zn–Fe alloy coatings become more corrosion resistant. For this

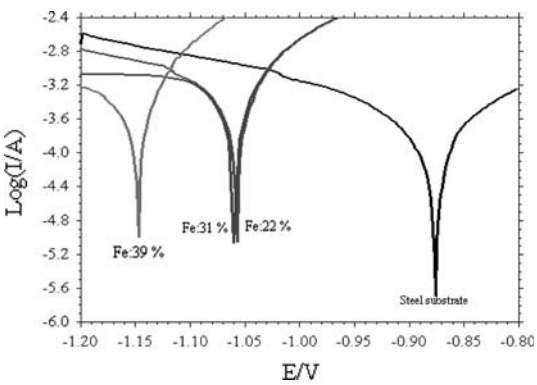

Fig. 5 Linear sweep voltammogram of electrodeposited Zn–Fe alloys and AISI 4140 substrate

purpose Zn–Fe coatings were investigated. Figure 5 shows the linear sweep voltammogram corresponding to the influence of iron content on the corrosion behavior of the electrodeposited Zn–Fe alloys. It can be seen that the free corrosion potentials of Zn–Fe alloys become more negative as the Fe content increases but a little negative than that of AISI 4140 steel substrate, which indicates that the Zn–Fe coating is an ideal anodic protective coating for iron or steel products, and can provide longer protection for iron or steel products than pure zinc coatings due to the smaller free corrosion potential difference between the Zn–Fe coating and that of iron-base substrate.

Conclusions

The protective Zn–Fe coatings were obtained from the acid sulfate bath. The corresponding electroplating behavior and corrosion properties of Zn–Fe alloys were investigated using cyclic voltammetry and linear sweep voltammetry methods. The effect of iron content was investigated on the electrical resistivity and the structure of Zn–Fe alloys, and the corrosion behavior of AISI 4140 steel substrates. The increase in the Fe content of plating bath enhanced the electrical conductivity and an increase in the Fe content promoted a decrease in the corrosion resistance of Zn–Fe deposit.

References

1. Zhang Z, Leng WH, Shao HB, Zhang JQ, Wang JM, Cao CN (2001) J Electroanal Chem 516:127
2. Fratesi R, Lunazzi G, Roventi G (1997) In: Fedrizzi L, Bonora PL (eds) Organic and inorganic coatings for corrosion prevention, vol. 20. The Institute of Materials, London, p 130
3. Rajagopalan SR (1972) Met Finish 70:52
4. Pushpavanam M, Natarajan SR, Balakrishnan K, Sharma LR (1991) J Appl Electrochem 21:642
5. Pech-Canul MA, Ramanauskas R, Maldonado L (1997) Electrochim Acta 42:255
6. Kautek W, Sahre M, Paatsch W (1994) Electrochim Acta 39:1151
7. Park H, Szpunar JA (1998) Corros Sci 40:525 c
8. Huang JF, Sun IW (2004) J Electrchem Soc 151(1):C8
9. Bajat JB, Miskovic-Stankovic VB, Kacarevic-Popovic Z (2004) Prog Org Coat 47(1):49
10. Bajat JB, Miskovic-Stankovic VB, Maksimovic MD, Drazic DM, Zec S (2004) J Serb Chem Soc 69(10):807
11. Brenner A (1963) Electrodeposition of alloys, vol. II. Academic Press, New York, p 194
12. Brenner A (1963) Electrodeposition of alloys, principle and practice, Chap. 31, vol. II. Academic Press, NewYork, p 239
13. Fletcher S (1983) Electrochim Acta 28:917
14. Miskovic-Stankovic VB, Zotovic JB, Kacarevic-Popovic Z, Maksimovic MD (1999) Electrochim Acta 44:4269
15. Bajat JB, Kacarevic-Popovic Z, Miskovic-Stankovic VB, Maksimovic MD (2000) Prog Org Coat 39:127
16. Powder Diffraction File, Inorganic Volume PD/S 5iRB, Sets 1–5,American Society for Testing and Materials, Philadelphia, PA, 1969
17. Adaniya T, Hara T, Sagiyama M, Homa T, Watanabe T (1985) Plat Surf Finish 72:52
18. Omar MA (1975) Elementary solid state physics. Addison-Wesley, Reading, p. 150